

Published in final edited form as:

*Int J Mass Spectrom.* 2012 December 15; 330-332: 220–225. doi:10.1016/j.ijms.2012.08.013.

## Protein structure evolution in liquid DESI as revealed by selective noncovalent adduct protein probing

Benjamin N. Moore, Omar Hamdy, and Ryan R. Julian\*

Department of Chemistry, University of California, Riverside, CA 92521, United States

### Abstract

Previous experiments based on charge state distributions have suggested that liquid desorption electrospray ionization (DESI) is capable of preserving solution phase protein structure during transfer to the gas phase (*Journal of the American Society for Mass Spectrometry* 21 (2010) 1730-1736). In order to examine this possibility more carefully, we have utilized selective non-covalent adduct protein probing (SNAPP) to evaluate protein structural evolution in both liquid DESI and standard ESI under a variety of conditions. Experiments with cytochrome c (Cytc) demonstrated that methanol induced conformational shifts previously observed with ESI are also easily observed with liquid DESI. However, undesirable acid-induced unfolding becomes apparent at very high concentrations of methanol in liquid DESI due to acetic acid in the spray solvent, suggesting that there are conditions under which liquid DESI will not preserve solution phase structure. The effects of ammonium acetate buffer on liquid DESI SNAPP experiments were examined by monitoring structural changes in myoglobin. Heme retention and SNAPP distributions were both preserved better in liquid DESI than traditional ESI, suggesting superior performance for liquid DESI in buffered conditions. Finally, liquid DESI SNAPP was used to study the natively disordered proteins  $\alpha$ ,  $\beta$ , and  $\gamma$  synuclein with SNAPP.  $\alpha$ -Synuclein, the main component of fibrils found in patients with Parkinson's disease, yielded a significantly different SNAPP distribution compared to  $\beta$  and  $\gamma$  synuclein. This difference is indicative of highly accessible protonated basic side chains, a property known to promote fibril formation in proteins.

### Keywords

Cytochrome c; Myoglobin; Synuclein; Charge residue; Ion evaporation

## 1. Introduction

Properly folded, biologically active proteins have secondary and tertiary structures essential to their role in the cell. A change in protein conformation is often associated with a change or loss in protein function. Determination of protein structure has been an area of interest especially given the therapeutic aspect of using small molecules or other conditions to activate, deactivate, or alter the function of proteins with the ultimate goal of treating disease. Traditionally, protein structure has been examined by solid and liquid phase techniques such as crystallography [1], NMR [2], FRET [3], fluorescence [4], and circular dichroism [5]. In recent years, mass spectrometry has been increasingly used to both directly and indirectly probe protein structure. Charge state distributions [6,7], selective non-covalent adduct protein probing (SNAPP) [8], covalent labeling [9], H/D exchange [10], ion mobility [11], electron capture dissociation (ECD) [12], and radical directed dissociation

(RDD) [13] have all been successfully used to examine protein structure and monitor how conformational changes occur in response to external stimuli. These mass spectrometry based techniques all rely on electrospray ionization (ESI), which is particularly important for those methods that examine protein structure in the gas phase. For experiments where protein structure is probed in vacuo, the ideal outcome is successful transfer of the solution phase structure into the gas phase with high fidelity. Unfortunately, conditions which favor this outcome typically reduce sensitivity significantly relative to standard ESI.

Recently, Chen and Miao reported that liquid DESI could be used to ionize proteins with apparent retention of solution-phase structure and enhanced sensitivity relative to ESI [14]. Liquid DESI, a technique related to solid surface DESI developed by Cooks and coworkers [15,16], consists of a simple experimental setup (see Fig. 1) where the sample and electrospray solutions are decoupled. The sample of interest is dissolved in one solution and pushed through a flat, open ended tube at a steady flow rate. A separate spray solvent, typically consisting of 50:50:1 water:methanol:acetic acid, is then electrosprayed and directed by high speed gas flow toward the sample solution tube. Charged droplets emerge from the intersection of the source and sample solutions, eventually generating protonated ions for detection in the mass spectrometer. Importantly, Chen and coworkers demonstrated that although denaturants such as methanol and acetic acid are used in the spray solvent, the protein charge states observed from liquid DESI ionization were similar to those obtained from much more “native” solutions [17]. In comparison, charge state distributions for proteins electrosprayed directly from 50:50:1 water:methanol:acetic acid exhibit significant shifts indicating denaturation of the protein. The apparent lack of denaturation in liquid DESI is of interest because decoupling the spray and sample solvents potentially enables maximization of ion count simultaneously with preservation of protein structure. However, subtle structural changes are difficult to detect by shifts in charge state distribution, suggesting that a more sensitive method may be required to reveal whether smaller changes in structure take place in liquid DESI.

SNAPP is a simple mass spectrometry based method for investigating protein structure that excels at identifying conformational changes. SNAPP is a comparative method that utilizes non-covalent attachment of probe molecules during ESI to monitor protein structure. SNAPP has been successfully used to reveal the effects of metal ions on the structure of  $\alpha$ -synuclein [18], to monitor structural changes induced by single amino acid mutations [19], and to distinguish small structural differences in highly homologous proteins from different species [20]. 18-Crown-6 (18C6) is typically the probe molecule used in SNAPP experiments due to its ability to non-covalently bind to the protonated side chains of lysine and arginine, or to the N-terminus. Side chains which are not buried or sequestered by intramolecular interactions are generally available to bind 18C6. Side chain availability is dictated by protein structure, and changes in protein conformation lead to different numbers of 18C6 adducts. In a typical experiment, 18C6 is simply added to a protein solution and then electrosprayed directly.

Herein, SNAPP will be utilized to examine the effects of the ionization process on protein structure for both liquid DESI and standard ESI. This work is the first use of SNAPP on proteins generated from a liquid DESI source. A methanol induced conformational shift in the protein cytochrome c (Cyt<sub>c</sub>) will be used as a model system to compare the two ionization processes. This system has been previously studied by SNAPP in ESI [8] and is examined here by SNAPP in liquid DESI. The protein structure of myoglobin ionized by liquid DESI from ammonium acetate buffer is examined by SNAPP to evaluate the performance of liquid DESI with additional buffer. The results with both Cyt<sub>c</sub> and myoglobin suggest that liquid DESI is a viable method for examining protein structure. Finally, liquid DESI is used to study dynamic structural differences in the natively

disordered synuclein proteins.  $\alpha$ -Synuclein is the principal component of amyloid fibrils associated with neurodegenerative Parkinson's disease and undergoes a high rate of fibril formation relative to the highly homologous proteins,  $\beta$  and  $\gamma$  synuclein [21]. Examination of these three proteins by liquid DESI SNAPP is performed in order to gain insight into the link between fibril formation rate and dynamic protein structure.

## 2. Experimental

Horse heart cytochrome c and myoglobin were purchased from Sigma–Aldrich (St. Louis, MO). The proteins  $\alpha$ ,  $\beta$ , and  $\gamma$  synuclein were purchased from ProSpecBio (East Brunswick, NJ). Distilled water was purified by a Millipore Direct-Q filtration system before use. Methanol, acetic acid, and ammonium acetate were purchased from Thermo-Fisher Scientific (Waltham, MA). 18-Crown-6 was purchased from Alfa Aesar (Pelham, NH).

### 2.1. ESI and DESI setup

All ESI spectra were acquired on a Thermo LTQ mass spectrometer with the standard IonMax™ ESI source supplied with the instrument. Liquid DESI spectra for myoglobin were acquired on a Thermo LTQ mass spectrometer and liquid DESI spectra for Cyt c were acquired on a Thermo LCQ mass spectrometer. The liquid DESI source was constructed in-house using a partially modified nozzle assembly from an existing Thermo ESI source. The assembly was modified by removing its enclosure and replacing the existing silica capillary (200  $\mu\text{m}$  O.D., 100  $\mu\text{m}$  I.D.) with a larger capillary (240  $\mu\text{m}$  O.D., 100  $\mu\text{m}$  I.D.) in order to increase sheath gas velocity at the spray tip. The spray assembly was properly grounded and attached to a firmly secured aluminum lab jack. The assembly was oriented in such a way that the emitted solvent plume impacted the flat cut end of a securely mounted portion of PEEK tubing (0.0625 in. O.D., 0.005 in. I.D.). A syringe pump was used to deliver sample solution through this tubing at 3  $\mu\text{L}/\text{min}$ . The samples consisted of 5  $\mu\text{M}$  protein and 100  $\mu\text{M}$  18C6 (1:20 ratio) in water unless otherwise noted. A second syringe pump was used to pump the spray solvent through the ESI needle at 3–6  $\mu\text{L}/\text{min}$ . The spray solvent consisted of 50:50:1 water:methanol:acetic acid unless otherwise noted. The nitrogen gas pressure going into the spray assembly was set to 80 psi. A picture of this setup is shown in Fig. 1. Sheath gas pressure, sample and spray flow rates, relative angles, and distances between the elements of the setup were optimized for ion count. For SNAPP experiments with both ion sources, ionization conditions and ion optic voltages were initially optimized to improve signal and 18C6 attachment to the protein. These conditions were then kept constant throughout the experiments. The optimal ion optic voltages were not substantially different between the two sources.

## 3. Results and discussion

Cyt c is known to undergo a conformational shift when exposed to increasing amounts of methanol [22], and is therefore an excellent test subject to examine the effects of ionization in liquid DESI. Fig. 2 shows fluorescence and circular dichroism spectra for solutions of Cyt c and 18C6 as a function of increasing methanol content at neutral pH. Cyt c contains a single tryptophan residue which fluoresces at 350 nm when excited at 285 nm. In the native protein structure this amino acid is buried within the hydrophobic core and does not fluoresce due to FRET quenching by the covalently bound heme group [22,23]. In Fig. 2a the measured fluorescence of Cyt c at 350 nm increases dramatically when the protein is exposed to >60% methanol. The increase in fluorescence results from a structural rearrangement increasing the distance between the tryptophan residue and heme group. The native fluorescence of the amino acid is shown as a control (red line) and is also noted to slightly decrease in intensity with increasing methanol content. Fig. 2b shows the circular

dichroism at 222 nm of Cytc under the same solvent conditions. Shifts in circular dichroism at 222 nm are also indicative of change in protein secondary structure. At 50–60% methanol, a significant shift toward increased helicity is observed. It is well known that the secondary structures of Cytc and many other proteins undergo conformational changes resulting in increased helicity when exposed to methanol and the changes observed here are in agreement with previous results [22,24].

SNAPP spectra of Cytc in varying amounts of methanol obtained by ESI and liquid DESI are shown in Fig. 3. Since SNAPP is a comparison technique, it is only relevant to compare data originating from the same ion source under the same operating conditions, meaning that direct comparison of individual ESI and DESI spectra is not meaningful. Rather, changes among the various DESI spectra can be compared to changes among the ESI spectra. For both liquid DESI and ESI, the number of 18C6 adducts increases substantially for the 50% methanol solution compared to the 0% methanol solution. This is consistent with the structural changes observed in solution in Fig. 2, although the transition is observed at a somewhat lower percentage of methanol (see supporting information). This is likely due to the stability of  $\alpha$ -helices in the gas phase, which may shift the balance of forces in favor of helix formation at a slightly lower percentage of methanol. There is not a dramatic shift in charge states for either the liquid DESI or ESI spectra at 50% methanol, although the charge states in both spectra are broadened somewhat. At 90% methanol, the ESI spectrum is very similar to that obtained at 50%; however, the liquid DESI spectrum has shifted notably toward higher charge states. This shift indicates that Cytc in liquid DESI is beginning to unfold at 90% methanol, a transition which is not expected to occur with just addition of methanol. The most likely explanation for this difference is the presence of acid in the liquid DESI spray solution. At lower concentrations of methanol, this acid is not sufficient to lead to denaturation of the protein within the timeframe of the experiment, which corresponds to the several milliseconds required to achieve complete desolvation [25,26]. After desolvation, the 18C6 adducts are locked in place and further changes to the SNAPP spectra are unlikely. However at 90% methanol, protein denaturation becomes feasible and leads to a partial shift of the charge state distribution [27]. It should be noted that the charge state distribution would be shifted substantially more if the acidic solution were sprayed directly, indicating that the liquid DESI source has still preserved some native structure even under these conditions.

Buffers are frequently added to ESI solutions in order to help preserve native structures [28,29], and could potentially counter the effects of adding acid to the liquid DESI spray solution. Liquid DESI and ESI SNAPP spectra for myoglobin in various concentrations of ammonium acetate buffer are shown in Fig. 4. When no buffer is present, both liquid DESI and ESI ionize the protein with 18C6 adducts attached, as expected. In ESI on the LTQ instrument a significant amount of apomyoglobin is observed, which is formed by loss of the noncovalently bound heme during ionization [30]. Heme loss is not prevalent in liquid DESI on the same instrument indicating a gentler ionization process [17]. ESI of myoglobin in the presence of buffer results in complete loss of 18C6 adducts even at the lowest concentration of buffer, as shown in Fig. 4f. With increasing buffer concentrations, the protein signal in ESI decreases significantly (Fig. 4, right). In contrast, 18C6 binding to the myoglobin decreases only slightly in liquid DESI as buffer concentration increases. Even at the maximum concentration of buffer examined, 1000  $\mu$ M, 18C6 adducts are still observable by liquid DESI.

Several competing factors influence the results in these experiments. 18C6 can form noncovalent complexes with any small cation, including ammonium. Given the relative concentrations of buffer and protein in these experiments, competitive binding of 18C6 by ammonium is unavoidable. In ESI, this leads to loss of all myoglobin–18C6 adducts,

although the  $[18C6+NH_4]^+$  peak becomes quite intense. Another important factor to consider is that there are a finite number of charges associated with each droplet in both ESI and liquid DESI. Therefore, if the number of charges consumed by one species increases, a corresponding decrease in charge consumption by another species must also occur. For ESI, it would appear that the addition of buffer leads primarily to generation of  $[18C6+NH_4]^+$ , accompanied by the decrease in myoglobin–18C6 formation. However in liquid DESI, 18C6 adducts to protein are still observed at high relative concentrations of buffer. Clearly a different mechanism is operating to generate ions in the case of liquid DESI. Let us consider the differences between the two sources more carefully. In ESI, the initially produced charged droplets go on to produce ions without significant further interaction with other solvents or surfaces. In liquid DESI, the charged droplets impact a surface, combine with another solution, and then depart from the surface. Charge transfer to the surface and dilution will serve to decrease charge density in the droplets which eventually go on to form ions in liquid DESI. In terms of the two extremes that are frequently invoked to describe the mechanism of ESI, charge residue and ion evaporation, dilution of charge will strongly favor the charge residue mechanism. The results suggest that, in ESI, charge partitioning due to ion evaporation of  $[18C6+NH_4]^+$  is significant and that insufficient 18C6 remains to form adducts with myoglobin. In liquid DESI, the data suggests that the charge residue mechanism dominates. Given that the protein is much more basic than ammonia, myoglobin is the eventual charge carrier in the shrinking residue droplet and is therefore able to compete for 18C6 adducts.

There are several important conclusions that can be drawn from the data in Fig. 4 with respect to liquid DESI and preservation of protein structure. One, liquid DESI does not appear to form ions via ion evaporation, which can lead to undesirable competitive losses in normal ESI. Two, the results imply that protein ions formed by the charge residue mechanism are more likely to retain native structures. This observation is important regardless of whether ESI or liquid DESI is to be employed and is in agreement with recent calculations [31]. Three, addition of buffer will likely counteract any denaturation induced by acid from the spray solvent.

Liquid DESI appears to be a viable method for gently ionizing proteins and appears to be well suited for SNAPP experiments. Therefore, we employed liquid DESI SNAPP to examine a novel system comprising the natively disordered proteins  $\alpha$ ,  $\beta$ , and  $\gamma$  synuclein. All three of the synuclein proteins are natively disordered meaning that they lack tertiary structure and rapidly interconvert between a variety of unique conformations.  $\alpha$ -Synuclein is known to be the principle component of fibril plaques present in Parkinson's disease [32–34].  $\beta$  and  $\gamma$  synuclein, although highly homologous to  $\alpha$ , are not related to the disease and form fibrils at significantly slower rates and have been shown to actually inhibit  $\alpha$ -synuclein fibril formation [35]. The disparity in fibril formation rates of the synuclein proteins suggests that transient structural properties may be key to explaining their observed biological activity.

Liquid DESI SNAPP distributions extracted from raw mass spectra are shown in Fig. 5 for each of the synucleins in the 14+, 13+, 12+, and 11+ charge states. In all charge states,  $\alpha$ -synuclein binds a significantly larger number of 18C6 molecules compared to both  $\beta$  and  $\gamma$  synuclein. This difference cannot be explained by primary sequence alone as these highly homologous proteins contain a similar number of potential 18C6 binding sites;  $\alpha$ -synuclein: 17,  $\beta$ -synuclein: 15,  $\gamma$ -synuclein: 18. Instead, it is likely that  $\alpha$ -synuclein can access a substantially different, perhaps more extended, set of conformations compared to  $\beta$  and  $\gamma$  synuclein. This difference in dynamic conformation may be related to the relatively high fibril formation rate of  $\alpha$ -synuclein.

An important factor in the ability of natively disordered proteins to oligomerize and form fibrils is the accessibility of their basic and acidic side chains [36]. At physiological pH, a protein with a high rate of aggregation will contain an equally large number of both positively and negatively charged residues that are solvent accessible and not participating in intramolecular electrostatic interactions. Intermolecular interactions can then cause the protein to form oligomers and eventually fibrils [37]. Binding of 18C6 is a direct indicator of this kind of protonated basic side chain accessibility. Therefore, it can be inferred that the increase in 18C6 binding to  $\alpha$ -synuclein relative to  $\beta$  and  $\gamma$  synuclein is reflective of the observed rates of fibril formation of the three proteins.

#### 4. Conclusion

The ability of liquid DESI to preserve solution phase protein structures has been examined. Protein conformation changes are observable with SNAPP in liquid DESI in a similar fashion to normal ESI SNAPP. Liquid DESI offers the advantage of higher ionization efficiency due to the use of an acidic spray solvent generally without denaturation of protein structure as would occur when using acidic spray solvent in ESI. In addition, liquid DESI was used to ionize protein in the presence of ammonium acetate buffer thus demonstrating the applicability of liquid DESI SNAPP under conditions that better reflect the cellular environment of proteins. Finally, liquid DESI was used to examine the natively disordered proteins  $\alpha$ ,  $\beta$ , and  $\gamma$  synuclein. Of the three proteins,  $\alpha$ -synuclein was shown to have a dynamic structure that bound a relatively large number of 18C6 molecules. The increased accessibility of protonated binding sites is likely related to the predisposition of  $\alpha$ -synuclein to undergo a high rate of fibril formation as compared to the other two synuclein proteins.

#### Supplementary Material

Refer to Web version on PubMed Central for supplementary material.

#### Acknowledgments

The authors thank NIH for funding (R01 GM084106).

#### References

1. Matthews BW. X-ray crystallographic studies of proteins. *Annual Review of Physical Chemistry*. 1976; 27:493–523.
2. Dyson HJ, Wright PE. Unfolded proteins and protein folding studied by NMR. *Chemical Reviews*. 2004; 104(8):3607–3622. [PubMed: 15303830]
3. Schuler B, Lipman EA, Eaton WA. Probing the free-energy surface for protein folding with single-molecule fluorescence spectroscopy. *Nature*. 2002; 419(6908):743–747. [PubMed: 12384704]
4. Vivian JT, Callis PR. Mechanisms of tryptophan fluorescence shifts in proteins. *Biophysical Journal*. 2001; 80(5):2093–2109. [PubMed: 11325713]
5. Chen YH, Yang JT, Martinez HM. Determination of secondary structures of proteins by circular-dichroism and optical rotatory dispersion. *Biochemistry*. 1972; 11(22):4120. [PubMed: 4343790]
6. Chowdhury SK, Katta V, Chait BT. Probing conformational-changes in proteins by mass-spectrometry. *Journal of the American Chemical Society*. 1990; 112(24):9012–9013.
7. Loo JA, Edmonds CG, Udseth HR, Smith RD. Effect of reducing disulfide-containing proteins on electrospray ionization mass-spectra. *Analytical Chemistry*. 1990; 62(7):693–698. [PubMed: 2327585]
8. Ly T, Julian RR. Using ESI-MS to probe protein structure by site-specific non-covalent attachment of 18-crown-6. *Journal of the American Society for Mass Spectrometry*. 2006; 17(9):1209–1215. [PubMed: 16766206]

9. Mendoza VL, Vachet RW. Probing protein structure by amino acid-specific covalent labeling and mass spectrometry. *Mass Spectrometry Reviews*. 2009; 28(5):785–815. [PubMed: 19016300]
10. Kaltashov IA, Eyles SJ. Studies of biomolecular conformations and conformational dynamics by mass spectrometry. *Mass Spectrometry Reviews*. 2002; 21(1):37–71. [PubMed: 12210613]
11. Bohrer BC, Mererbloom SI, Koeniger SL, Hilderbrand AE, Clemmer DE. Biomolecule analysis by ion mobility spectrometry. *Annual Review of Analytical Chemistry*. 2008; 1:293–327.
12. Oh H, Breuker K, Sze SK, Ge Y, Carpenter BK, McLafferty FW. Secondary and tertiary structures of gaseous protein ions characterized by electron capture dissociation mass spectrometry and photofragment spectroscopy. *Proceedings of the National Academy of Sciences of the United States of America*. 2002; 99(25):15863–15868. [PubMed: 12444260]
13. Ly T, Julian RR. Elucidating the tertiary structure of protein ions in vacuo with site specific photoinitiated radical reactions. *Journal of the American Chemical Society*. 2010; 132(25):8602–8609. [PubMed: 20524634]
14. Miao ZX, Chen H. Direct analysis of liquid samples by desorption electrospray ionization-mass spectrometry (DESI-MS). *Journal of the American Society for Mass Spectrometry*. 2009; 20(1): 10–19. [PubMed: 18952458]
15. Takats Z, Wiseman JM, Gologan B, Cooks RG. Mass spectrometry sampling under ambient conditions with desorption electrospray ionization. *Science*. 2004; 306(5695):471–473. [PubMed: 15486296]
16. Venter A, Sojka PE, Cooks RG. Droplet dynamics and ionization mechanisms in desorption electrospray ionization mass spectrometry. *Analytical Chemistry*. 2006; 78(24):8549–8555. [PubMed: 17165852]
17. Miao ZX, Wu SY, Chen H. The study of protein conformation in solution via direct sampling by desorption electrospray ionization mass spectrometry. *Journal of the American Society for Mass Spectrometry*. 2010; 21(10):1730–1736. [PubMed: 20620076]
18. Ly T, Julian RR. Protein–metal interactions of calmodulin and alpha-synuclein monitored by selective noncovalent adduct protein probing mass spectrometry. *Journal of the American Society for Mass Spectrometry*. 2008; 19(11):1663–1672. [PubMed: 18691903]
19. Liu ZJ, Cheng SJ, Gailie DR, Julian RR. Exploring the mechanism of selective noncovalent adduct protein probing mass spectrometry utilizing site-directed mutagenesis to examine ubiquitin. *Analytical Chemistry*. 2008; 80(10):3846–3852. [PubMed: 18407670]
20. Tao YQ, Julian RR. Examining protein surface structure in highly conserved sequence variants with mass spectrometry. *Biochemistry*. 2012; 51(8):1796–1802. [PubMed: 22320248]
21. Dauer W, Przedborski S. Parkinson's disease: mechanisms and models. *Neuron*. 2003; 39(6):889–909. [PubMed: 12971891]
22. Kamatari YO, Konno T, Kataoka M, Akasaka K. The methanol-induced globular and expanded denatured states of cytochrome c: a study by CD fluorescence, NMR and small-angle X-ray scattering. *Journal of Molecular Biology*. 1996; 259(3):512–523. [PubMed: 8676385]
23. Tsong TY. Ferricytochrome-c chain folding measured by energy-transfer of tryptophan 59 to heme group. *Biochemistry*. 1976; 15(25):5467–5473. [PubMed: 11814]
24. Bhakuni V. Alcohol-induced molten globule intermediates of proteins: are they real folding intermediates or off pathway products? *Archives of Biochemistry and Biophysics*. 1998; 357(2): 274–284. [PubMed: 9735168]
25. Breuker K, McLafferty FW. Stepwise evolution of protein native structure with electrospray into the gas phase, 10(–12) to 10(2) S. *Proceedings of the National Academy of Sciences of the United States of America*. 2008; 105(47):18145–18152. [PubMed: 19033474]
26. Kebarle P, Verkerk UH. Electrospray from ions in solution to ions in the gas phase, what we know now. *Mass Spectrometry Reviews*. 2009; 28(6):898–917. [PubMed: 19551695]
27. Konermann L, Douglas DJ. Acid-induced unfolding of cytochrome c at different methanol concentrations: electrospray ionization mass spectrometry specifically monitors changes in the tertiary structure. *Biochemistry*. 1997; 36(40):12296–12302. [PubMed: 9315869]
28. Verkerk UH, Peschke M, Kebarle P. Effect of buffer cations and of H<sub>3</sub>O<sup>+</sup> on the charge states of native proteins. Significance to determinations of stability constants of protein complexes. *Journal of Mass Spectrometry*. 2003; 38(6):618–631. [PubMed: 12827631]

29. Loo JA, Loo RRO, Andrews PC. Primary to quaternary protein-structure determination with electrospray-ionization and magnetic-sector mass-spectrometry. *Organic Mass Spectrometry*. 1993; 28(12):1640–1649.
30. Wang X, Zhao WJ, Lin X, Su B, Liu JF. Observation of symmetric denaturation of hemoglobin subunits by electrospray ionization mass spectrometry. *Journal of Mass Spectrometry*. 2010; 45(11):1306–1311. [PubMed: 20963788]
31. Ahadi E, Konermann L. Modeling the behavior of coarse-grained polymer chains in charged water droplets: implications for the mechanism of electrospray ionization. *Journal of Physical Chemistry B*. 2012; 116(1):104–112.
32. Lee JC, Langen R, Hummel PA, Gray HB, Winkler JR. Alpha-synuclein structures from fluorescence energy-transfer kinetics: implications for the role of the protein in Parkinson's disease. *Proceedings of the National Academy of Sciences of the United States of America*. 2004; 101(47):16466–16471. [PubMed: 15536128]
33. Polymeropoulos MH, Lavedan C, Leroy E, Ide SE, Dehejia A, Dutra A, Pike B, Root H, Rubenstein J, Boyer R, Stenroos ES, Chandrasekharappa S, Athanassiadou A, Papapetropoulos T, Johnson WG, Lazzarini AM, Duvoisin RC, DiIorio G, Golbe LI, Nussbaum RL. Mutation in the alpha-synuclein gene identified in families with Parkinson's disease. *Science*. 1997; 276(5321):2045–2047. [PubMed: 9197268]
34. Dawson TM, Dawson VL. Molecular pathways of neurodegeneration in Parkinson's disease. *Science*. 2003; 302(5646):819–822. [PubMed: 14593166]
35. Sung YH, Eliezer D. Residual structure, backbone dynamics, and interactions within the synuclein family. *Journal of Molecular Biology*. 2007; 372(3):689–707. [PubMed: 17681534]
36. Fandrich M, Forge V, Buder K, Kittler M, Dobson CM, Diekmann S. Myoglobin forms amyloid fibrils by association of unfolded polypeptide segments. *Proceedings of the National Academy of Sciences of the United States of America*. 2003; 100(26):15463–15468. [PubMed: 14665689]
37. Picotti P, De Franceschi G, Frare E, Spolaore B, Zambonin M, Chiti F, de Laureto PP, Fontana A. Amyloid fibril formation and disaggregation of fragment 1–29 of apomyoglobin: insights into the effect of pH on protein fibrillogenesis. *Journal of Molecular Biology*. 2007; 367(5):1237–1245. [PubMed: 17320902]

## Appendix A. Supplementary data

Supplementary data associated with this article can be found, in the online version, at <http://dx.doi.org/10.1016/j.ijms.2012.08.013>.



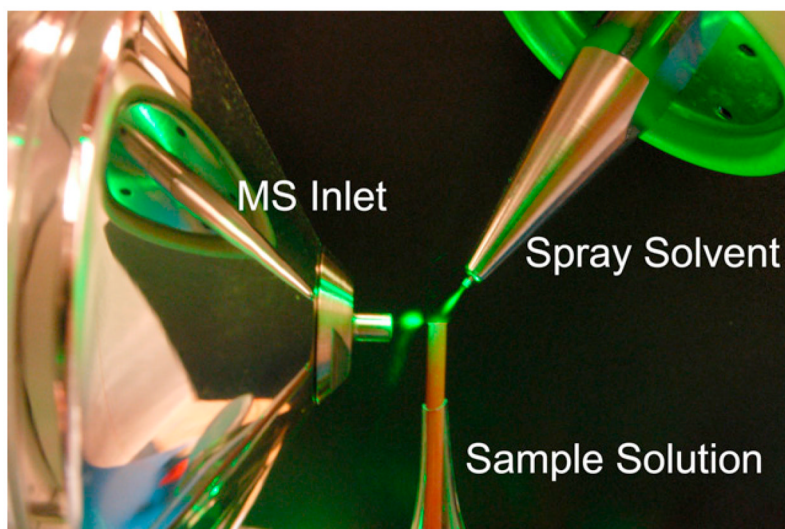


**Fig. 1.** Composite image of the liquid DESI source setup. A green laser pointer is used to illuminate the droplet clouds between the ionization source, sample tube, and mass spectrometer inlet. (For interpretation of the references to color in this figure legend, the reader is referred to the web version of the article.)

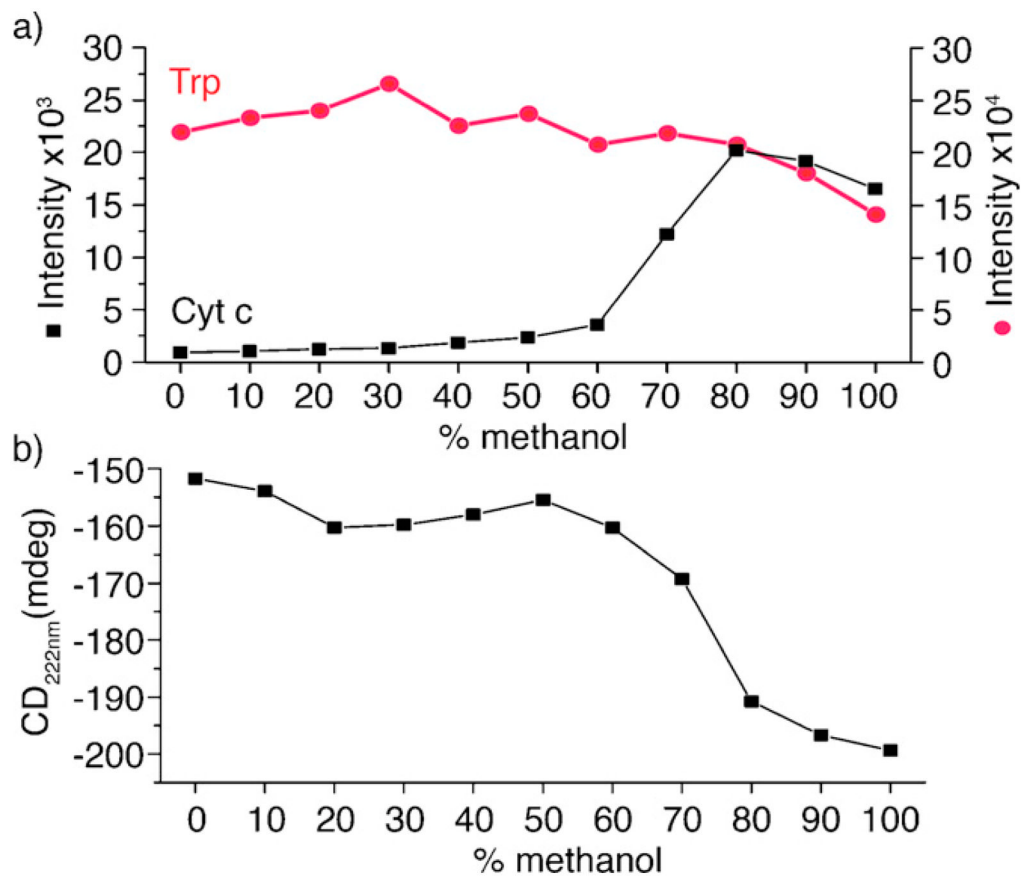


**Fig. 2.** (a) Fluorescence at 350 nm of Cyt c and tryptophan and (b) circular dichroism at 222 nm of Cyt c in increasing concentrations of methanol. (For interpretation of the references to color in text, the reader is referred to the web version of the article.)



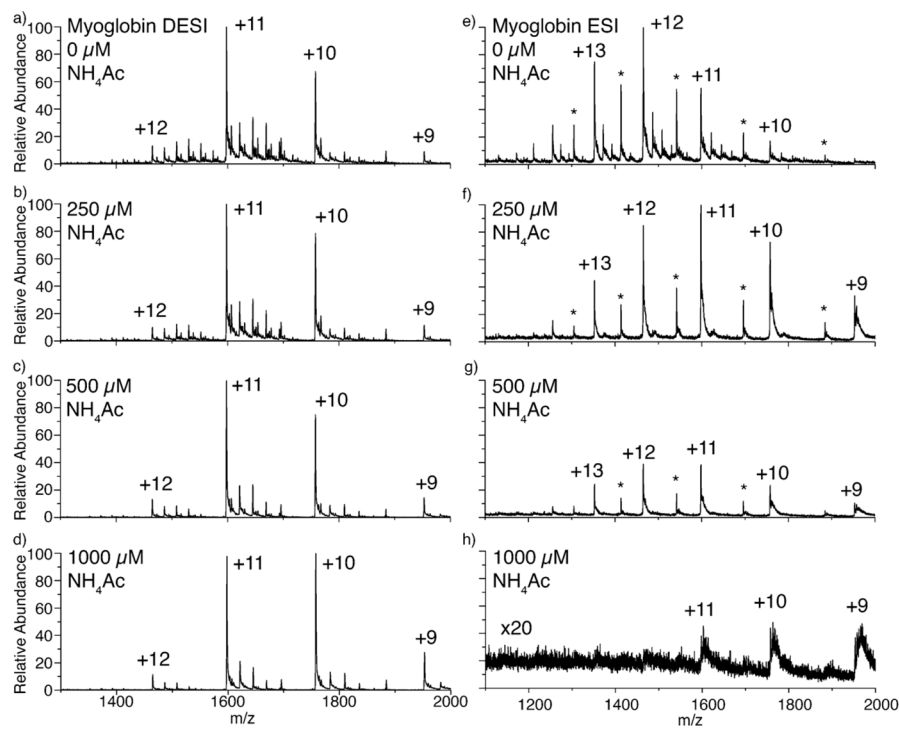


**Fig. 4.** Solutions of the protein myoglobin with increasing concentrations of ammonium acetate buffer ionized via (a–d) DESI and (e–h) ESI.

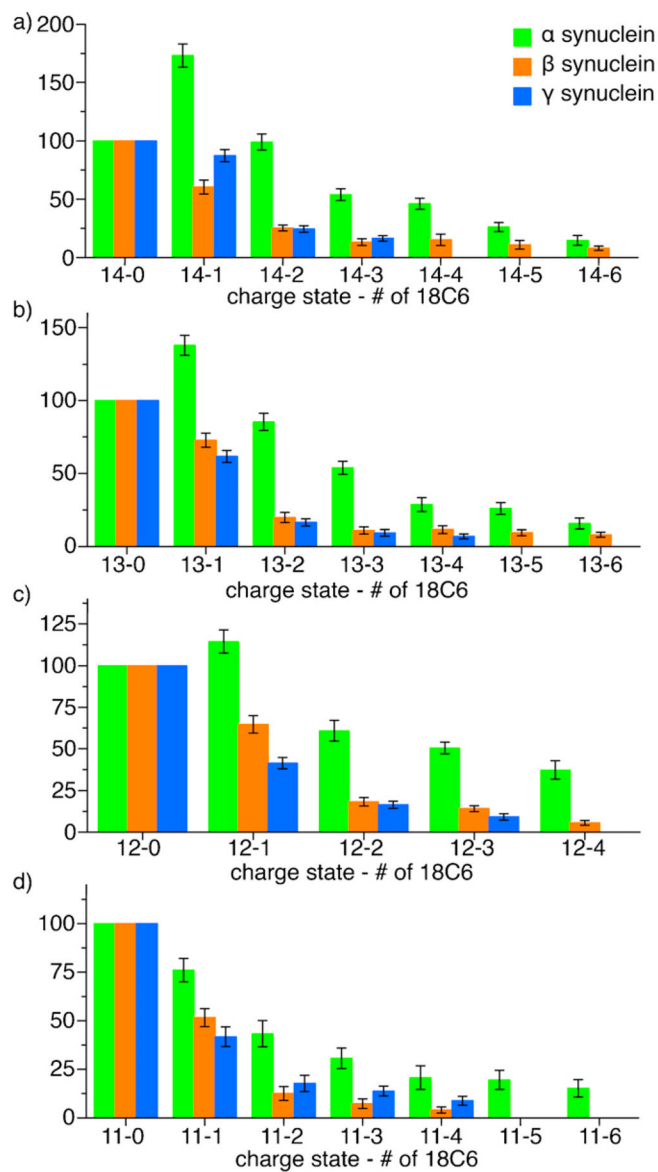


**Fig. 5.** SNAPP distributions of  $\alpha$ ,  $\beta$ , and  $\gamma$  synucleins in  $H_2O$  via DESI.